

The enigmatic WR46: A binary or a pulsator in disguise*

I. The photometry

P. M. Veen¹, A. M. van Genderen¹, K. A. van der Hucht², W. H. Allen³, T. Arentoft⁴, and C. Sterken^{4, **}

¹ Leiden Observatory, Postbus 9513, 2300 RA Leiden, The Netherlands

² Space Research Organization Netherlands, Sorbonnelaan 2, 3584 CA Utrecht, The Netherlands

³ Vintage Lane Observatory (RASNZ), 456 D Vintage Lane, RD 3, Blenheim, New Zealand

⁴ Astronomy Group, Free University of Brussels (VUB), Pleinlaan 2, 1050 Brussels, Belgium

Received 1 September 2000 / Accepted 5 November 2001

Abstract. We discuss the observational history of the Wolf-Rayet object WR 46 (WN3p), including a re-investigation of the original discovery plates from early this century. We find that the reported presence of N III lines is a mis-interpretation of N V lines and conclude that the object did not change its spectral type since the first recording one century ago. We performed photometric monitoring in the period 1986–1999, and confirm that the object shows cyclical variability on a time scale of hours. The shape of the light curves varies from purely sinusoidal to irregular, and from an amplitude of nearly $0.^m 1$ to constancy. In addition, night-to-night variability of the mean brightness causes folded light curves to display a large scatter. We investigate the frequency behaviour of the photometric data. From the periodograms of our two large data sets, in 1989 and in 1991, we identify frequencies of significantly different values 7.08 cd^{-1} and 7.34 cd^{-1} , respectively. Moreover, the 1989 data show strong evidence for an additional frequency $f_x = 4.34 \text{ cd}^{-1}$. The periodograms of our eight smaller data sets show more ambiguous behaviour. We discuss whether these latter data show evidence for multi-frequency behaviour, or whether they can be reconciled with a single clock with a changing clock-rate. As pointed out by van Genderen et al. (1991), if the data are folded using twice the single-wave period, the light curves appear ellipsoidal with unequal minima. Although the difference in depth of the minima is hardly significant, it does occur in both large data sets. Moreover, the simultaneously obtained radial velocity measurements are in better agreement with the double-wave than the single-wave period (Paper II). Finally, Marchenko et al. (2000) observed WR 46 to have a single-wave period of the same order as the double-wave period identified here. The periodograms of the ($V-W$) colour index show that the colour changes are controlled by single-wave frequencies, or their sub-harmonics (double-wave periods), but not by f_x . The colour variation of WR 46 is peculiar in the sense that the object is red when bright and blue when faint. Although the spectrum of WR 46 has been suggested to originate from a stellar disc, this peculiar colour behaviour is in line with its WR nature, which is also confirmed by its spectral variability (Marchenko et al. 2000; Paper II). In addition, our seasonal photometric averages of WR 46 show a rise from 1989 to 1991 of $0.^m 12$, confirming the brightening detected by the *Hipparcos*-satellite (Marchenko et al. 1998). Eventually, WR 46 brightened by about $0.^m 25$ and subsequently declined on a time scale of years. Such a rise is unique among the WR stars in the *Hipparcos*-survey, and has not been found anywhere else. We investigate the changes to the double-wave behaviour and mean colour-index coinciding with the period change and brightening. Interpretation of the object as either a multi-frequency non-radial WR pulsator, or a WR binary with possible large orbital decay is deferred to Paper III.

Key words. stars: Wolf-Rayet – stars: individual: WR 46 – stars: binaries: close – stars: variables: general – stars: oscillations

1. Introduction

The Wolf-Rayet (WR) object WR 46 = HD 104994 = DI Cru (WN3p) shows remarkable variability. Its short-term variability seems to be driven by a low-mass close

companion (van Genderen et al. 1991), but a large period change casted considerable doubt upon that interpretation (Veen et al. 1999). In addition, *Hipparcos* revealed long-period variability (Marchenko et al. 1998). Therefore, we re-investigate our data and other data available to us in order to study correlations with the long-term behaviour and find clues to the origin of the variability.

The present paper, the first in a series of three, discusses the observational history of WR 46 and presents monitoring photometry, partly published before, and in

Send offprint requests to: A. M. van Genderen,
e-mail: genderen@strw.leidenuniv.nl

* Largely based on observations collected at the European Southern Observatory (ESO), La Silla, Chile.

** Belgian Fund for Scientific Research (FWO).

part newly obtained data. We investigate its cyclical short-term variability and the intriguing long-term photometric behaviour of the object. In Veen et al. (2002a) (hereafter Paper II) we present simultaneously obtained spectroscopy and search for confirmation of the photometric periods. We discuss the line-flux and radial-velocity curves when folding with the identified periods. The apparent time-delays between the different emission lines confirm the stratified nature of the WR stellar wind. Because the interpretation remains ambiguous, it is presented completely separate in a third paper (Veen et al. 2002b; hereafter Paper III). In addition to a binary model, non-radial pulsation is also discussed as a possible origin of the variability. Moreover, the variability is compared to other short-periodic variable WR stars. Finally, Veen & Wieringa (2000) present upper limits to the radio flux of WR 46.

2. Observational history

As given in the bibliography accompanying the VIth Galactic Wolf-Rayet Catalogue (van der Hucht et al. 1981), the object WR 46 was first recognized as a WR-like object by Fleming (1910, 1912) and listed as CPD–61°2945. She measured the objective prism plates of the Henry Draper Memorial, and derived a magnitude of 9^m6. Cannon (1916) describes the spectrum of CPD–61°2945 as follows: “*The spectrum appears to consist of two bright lines at 4686 and 4638, of nearly equal intensity, and superposed on a strong continuous spectrum*”. However, since the early fifties (Smith 1955) the spectrum shows, next to the He II 4686 line, the N V line at 4604–19 Å instead of the N III line at 4638 Å. Therefore, we re-investigated the old photographic plates.

Three early plates (1899, 1902, 1908) of the Harvard Observatory collection with a spectrum of WR 46 were recovered for us by Dr. M. Hazen. Polaroid photographs were taken from these originals with an enlargement of a factor three. The 1908 plate used by Cannon (B38828 = #333 in her numbering) has a resolution of $\sim 500 \text{ \AA mm}^{-1}$ and shows the object vaguely. However, on the discovery plate of 1899 with a resolution of 140 \AA mm^{-1} the spectrum clearly shows a line 75 (± 10) Å shortward of the bigger He II 4686 line, confirming the N V line identification. The 1902 plate (A5798) also has the higher resolution, but shows the object very faint. Yet, it seems to confirm the N V identification. Therefore, we assume that Cannon, possibly also in other cases (e.g., the WN3 star WR 152), has mistaken the N V line for the N III line. This is understandable because of the low spectral resolution of her plates, especially since the possibility of a line occurring at around 4610 Å due to N V may not have been known to her. The persistent nature of the N V emission lines and of the low intensity of the He-Pickering lines leads us to conclude that WR 46 did not change its spectral type since then. Note, however, that Paper II deals with (cyclic) variability of various emission lines.

Payne (1930) questioned the WR nature of WR 46 by classifying it as W? without any further comment.

Table 1. Optical photometric observations of WR 46 as listed by van der Hucht et al. (1981) plus more recent data.

mag.	spectr.	reference
	type	
pg 9.6	V	Fleming (1910, 1912) (CPD–61°2945)
	Ocp	Cannon (1916) (CPD–61°2945)
pg 10.4	Ocp	Wilson & Luyten (1925)
pg 10.1	W?c	Payne (1930)
pg 9.9		Münch (1953) (123e = CD – 61°3331)
pg 10.1	WN5p	Smith (1955)
V 10.4		<i>ibid.</i>
	WN4p	Roberts (1962) (MR 40)
v 10.96	WN3	Smith (1968b) (suspects var.)
pg 10.6		Stephenson & Sanduleak (1971)
V 10.93		Lynga & Wramdemark (1973)
B 10.87		<i>ibid.</i>
U 10.03		<i>ibid.</i>
	WN4	Henize (1976) (He3-749)
V _{ANS} 10.86	WN3	van de Hucht et al. (1979)
	WN3p	van der Hucht et al. (1981) (WR 46)
v 10.87		Torres-Dodgen & Massey (1988)
V 10.82		Westerlund & Garnier (1989)
B 10.79		<i>ibid.</i>
U 9.95		<i>ibid.</i>
<i>m</i> ₁₆₄₀ 7.7		Tovmassian et al. (1996)
H _p 10.9		Marchenko et al. (1998) (var.)

Smith (1955) was the first to publish a spectrum of WR 46 and noted the presence of emission lines O VI 3811–34, leading to its label “peculiar”. Another spectrum was presented by Smith (1968a) showing only its line complex around 4650 Å. In her photometric investigation of WR stars Smith (1968b) suspects WR 46 to be variable. Table 1 summarizes most previous photometric investigations and identifications of WR 46. Furthermore, WR 46 has been investigated for circumstellar nebulosity by Marston et al. (1994), who found none in H α within a region of $31' \times 31'$. Discussion on the distance of the object is given by Veen & Wieringa (2000) and van der Hucht (2001).

The first evidence of short-term photometric variability by WR 46 was presented by Monderen et al. (1988). Based on additional photometric monitoring obtained in 1988 and 1989, van Genderen et al. (1991) demonstrated that, if phased with a period of 0.2824 d ($f = 3.541 \text{ cd}^{-1}$), the light- and colour-curves show a double-wave with an amplitude in V of 0^m1. In that paper the variation is considered to be due to rotation of a distorted star in a close binary system. The ratio of the depths of both minima was interpreted as a measure ($\sim 10\%$ in size) of the distortion of the luminous WR component. The scatter around the mean light curve amounting to 0^m07 was ascribed to instability of the continuum forming layer.

A preliminary radial-velocity curve was also presented and later discussed in more detail by Verheijen (1991). Van Genderen et al. (1991) suggested that the companion of the WR star could be a low-mass object, possibly a compact object.

Veen et al. (1995) and Niemela et al. (1995) confirmed the radial-velocity variability of WR 46, though with a larger amplitude. Furthermore, long-term variability, unique among the WR stars, is uncovered from photometry by the *Hipparcos*-satellite during 1989–1993 (Marchenko et al. 1998; see Fig. 13 of the present paper). Veen et al. (1999) suggested that such long-term brightenings are recurrent and showed that a similar behaviour is also evident in the equivalent widths (*EW*) of the emission lines (see also Paper II).

Crowther et al. (1995, hereafter CSH) applied their non-LTE “WR standard model” to WR 46, analyzing its ultraviolet, optical and infrared spectrum. The results are similar to those obtained by Schmutz et al. (1989), Hamann et al. (1995a), and Hamann & Koesterke (1998). CSH concluded that the group of *weak-lined* WNE stars, to which WR 46 belongs, are as hot and luminous as the *strong-lined* WNE stars, but with lower mass-loss rates by an order of magnitude. Moreover, the position of WR 46 itself in the theoretical HR-diagram seems outstanding since it appears even hotter and brighter, and thus beyond any evolutionary track of single WR stars (see their Fig. 9).

In line with the suggestion by Niemela et al. (1995), Steiner & Diaz (1998) proposed WR 46 to be a member of a class of evolved hot emission-line binary systems, so-called “V Sagittae stars”, newly introduced by these authors. In their view, this class consists of four objects (including the prototype) two of which are also classified as WR stars, viz. WR 46 and WR 109. Their class is suggested to be related to the Super Soft X-ray Sources (SSS), where accretion discs feature prominently. Discussion about this controversy is deferred to Paper II.

3. Observations and reduction

3.1. Walraven photometry

Between 1986 and 1991, observations of WR 46 were obtained using the Dutch 90-cm telescope at ESO (La Silla, Chile) equipped with the simultaneous five-colour photometer of Walraven (*VBLUW*). The photometric system is described by Lub & Pel (1977) and details on the pass-bands are given by de Ruiter & Lub (1986). The data were obtained by different observers as listed in Table 2. WR 46 was observed together with WR 50 (LSS 3013 = TH 17 – 84, WC7+a), both relative to the comparison star HD 108355 (HR 4736, B8 IV), as follows: sky–C–46–50–C–46–50–C–sky, etc. (except for the only night in 1986 by Monderen et al. 1988). The observations of WR 50 will not be discussed here. Integration times were 30 s for the comparison star and 2 min for the program stars and the sky background. The aperture was 16''.5. All data were calibrated by means of standard stars measured throughout each night.

The mean photometric properties of the comparison star are listed in Table 3. For each data set we list the mean magnitudes and colours of WR 46 in Table 2. The relatively large standard deviations for WR 46, especially in *V*, reflect its variability. The photometric parameters in the Walraven system are in log *I* scale (i.e., magnitudes divided by –2.5). Throughout this paper magnitudes will be indicated explicitly using superscript “m”. For normal absorption-line stars the Walraven scale can be transformed to Johnson *V_J* and *(B – V)_J* by the formulae of Pel (1986):

$$\begin{aligned} V_J &= 6^{\text{m}}.886 - 2.5[V + 0.033(V - B)] \\ (B - V)_J &= 2.571(V - B) - 1.020(V - B)^2 \\ &\quad + 0.500(V - B)^3 - 0^{\text{m}}.010. \end{aligned}$$

However, for an emission-line object like WR 46, systematic differences can be introduced of the order of a few tenths of a magnitude (see also Duijsens et al. 1996 on WR 6). The *V_J* and *(B – V)_J* values are only meaningful for the comparison star HD 108355 (cf. Table 3).

The photometric quality of each night was judged from a large number of observations of other program and comparison stars. Furthermore, every single observation made by the Walraven photometer is split into two halves and the difference between them is a measure of the quality. Based on this we rejected several data points. The resulting light curves for the *V*-band are shown in Fig. 1 (1988–1990) and Fig. 2 (1991).

3.2. *U_CV₉₉R₁₉₄* single channel photometry

In April 1995, the Walraven photometer was dismantled, and we used the ESO 50-cm telescope with a single channel photometer. We obtained differential magnitudes relative to HD 105150 (A0/1 V) (Slawson et al. 1992, see Table 3). We used the Cousins *U_C* (ESO#556) filter, and the *V*(ESO#99) and *R*(ESO#194) filters, which were selected to receive mostly continuum light (see Fig. 14). We used the differential *V* magnitude to approximate the absolute *V_J* magnitude as listed in Table 3. The atmospheric extinction information was supplied by Burki (1996, private communication). The resulting *V* light curve in magnitudes is shown in Fig. 3.

3.3. *(UVR)_B* CCD photometry

In February and May 1998 the Dutch 90-cm telescope was used again, now with a CCD (ESO#33) photometer attached. The standard Bessel *U_B*(ESO#634), *V_B*(ESO#420), *R_B*(ESO#421) filters of the Dutch telescope were used. We also observed the comparison star HD 105150 in order to link the photometry to the observations from 1995. We performed differential photometry with respect to stars within the CCD-frame (Fig. 4). The mean values are listed in Table 3 and the resulting *V* light curves are presented in Figs. 5 and 6.

Table 2. Summary of our photometric observations of WR 46. Column 1 lists the names of the observers and the identification of the data sets. Large data sets are printed in boldface. “(S)” indicates that in three or four nights simultaneous spectra were obtained (see Paper II). Columns 2 and 3 list the first and last night of the observing run and on the second line the actual number of nights and the total number of data points per filter. For the data sets up to 1991 the mean absolute photometric parameters in the Walraven *VBLUW* system ($\log I$) and Johnson V_J and $(B - V)_J$ (in magnitude scale) are listed. Also indicated is the standard deviation (σ), which represents typically the stellar variability and the instrumental scatter for the colours within one night. For the 1995 data set differential photometric parameters are listed with respect to HD 105150 (see Table 3) in a selected *UVR* filter set (see text). For both data sets in 1998 we list the differential Bessel *UVR* magnitudes. Part of the data is discussed elsewhere, as indicated by footnotes to the table. The last column lists the time of phase zero: $T_0 = \text{HJD}(\phi_0) - 24\,40\,000$.

Observer data set	epoch		V	$V - B$	$B - U$	$U - W$	$B - L$	V_J	$(B - V)_J$	T_0
	#nights	#points	σ_V	σ_{V-B}	σ_{B-U}	σ_{U-W}	σ_{B-L}	σ_V	σ	
P. Monderen ^{a,b} (1986)	13-04	14-04-86	-1.623	0.042	-0.050	-0.027	-0.025	10 ^m .94	0 ^m .097	
	1	19	0.010	0.002	0.002	0.004	0.003	0 ^m .025	0 ^m .005	
I. Larsen ^c (1988)	13-02	22-02-88	-1.628	0.044	-0.049	-0.021	-0.022	10 ^m .95	0 ^m .101	7204.01
	3	93	0.014	0.003	0.004	0.005	0.003	0 ^m .034	0 ^m .007	
E. Kuulkers ^d (1989-I)	08-02	11-02-89	-1.619	0.043	-0.041	-0.023	-0.014	10 ^m .93	0 ^m .098	7566.04
	4	94	0.010	0.004	0.005	0.009	0.004	0 ^m .024	0 ^m .009	
E. van Kampen^d (1989-II)(S)	11-03	20-03-89	-1.619	0.045	-0.044	-0.021	-0.017	10^m.93	0^m.104	7566.04
	9	361	0.011	0.003	0.003	0.004	0.004	0^m.027	0^m.006	
J.P. de Jong (1990)(S)	28-02	08-03-90	-1.620	0.042	-0.042	-0.025	-0.015	10 ^m .93	0 ^m .096	7951.16
	8	279	0.014	0.006	0.006	0.015	0.005	0 ^m .035	0 ^m .014	
O. Kolkman (1991-I)	23-01	31-01-91	-1.594	0.046	-0.046	-0.026	-0.017	10 ^m .87	0 ^m .106	8280.01
	9	80	0.015	0.005	0.006	0.012	0.006	0 ^m .039	0 ^m .013	
M. Verheijen (1991-II)(S)	01-02	01-03-91	-1.571	0.044	-0.041	-0.026	-0.009	10^m.81	0^m.100	8280.01
	25	473	0.020	0.003	0.004	0.005	0.005	0^m.050	0^m.009	
			<u>ΔV_{99}</u>	<u>ΔU_C</u>	<u>ΔR_{194}</u>					
M. Duijsens (1995)(S)	02-04	05-04-95	3 ^m .17	2 ^m .34	3 ^m .19			10 ^m .84		9811.25
	4	67	0 ^m .03	0 ^m .02	0 ^m .03					
			<u>ΔV_B</u>	<u>ΔU_B</u>	<u>ΔR_B</u>					
M. Janson (1998-I)(S)	10-02	12-02-98	-1 ^m .25	-4 ^m .01	-0 ^m .77			10 ^m .78		10 855.04
	3	20	0 ^m .03	0 ^m .03	0 ^m .03					
P. de Wildt (1998-II)	13-05	01-06-98	-1 ^m .15	-3 ^m .92	-0 ^m .60			10 ^m .88		10 947.14
	6	113	0 ^m .04	0 ^m .03	0 ^m .05					
T. Arentoft/C.S. ^e (1999-I)	01-01	31-01-99	-1 ^m .22					10 ^m .81		-
	8/12	23	0 ^m .04							
C.Sterken ^e (1999-II)	24-03	01-04-99	-1 ^m .29					10 ^m .74		-
	9	109	0 ^m .05							
			<u>ΔV_J</u>							
B. Allen (1999-III)	12-04	19-04-99	-0 ^m .09					10 ^m .85		11 280.61
	2	797	0 ^m .04							

^a Monderen et al. (1988); ^b Lub (1999), private communication; ^c van Genderen et al. (1990); ^d van Genderen et al. (1991); ^e Marchenko et al. (2000) (C.S. signifies C. Sterken).

Table 3. Photometric parameters in the Walraven *VBLUW* system are listed for the comparison star HD 108355. The second row lists the standard deviation. Transformation to Johnson magnitudes is in agreement with the determination by Slawson et al. (1992). For the comparison star HD 105150, used in 1995 and 1998, Johnson magnitudes determined by Slawson et al. (1992) are listed. The Walraven measurements are in agreement with de Geus et al. (1990).

star	spectral class	V	$V - B$	$B - U$	$U - W$	$B - L$	V_J	$(B - V)_J$
		σ_V	σ_{V-B}	σ_{B-U}	σ_{U-W}	σ_{B-L}	σ	σ
HD 108355	B8 IV	0.342	0.036	0.255	0.073	0.085	6 ^m .03	0 ^m .081
		0.003	0.002	0.002	0.002	0.002	0 ^m .008	0 ^m .005
HD 105150	A0/1 V						7 ^m .67	0 ^m .11

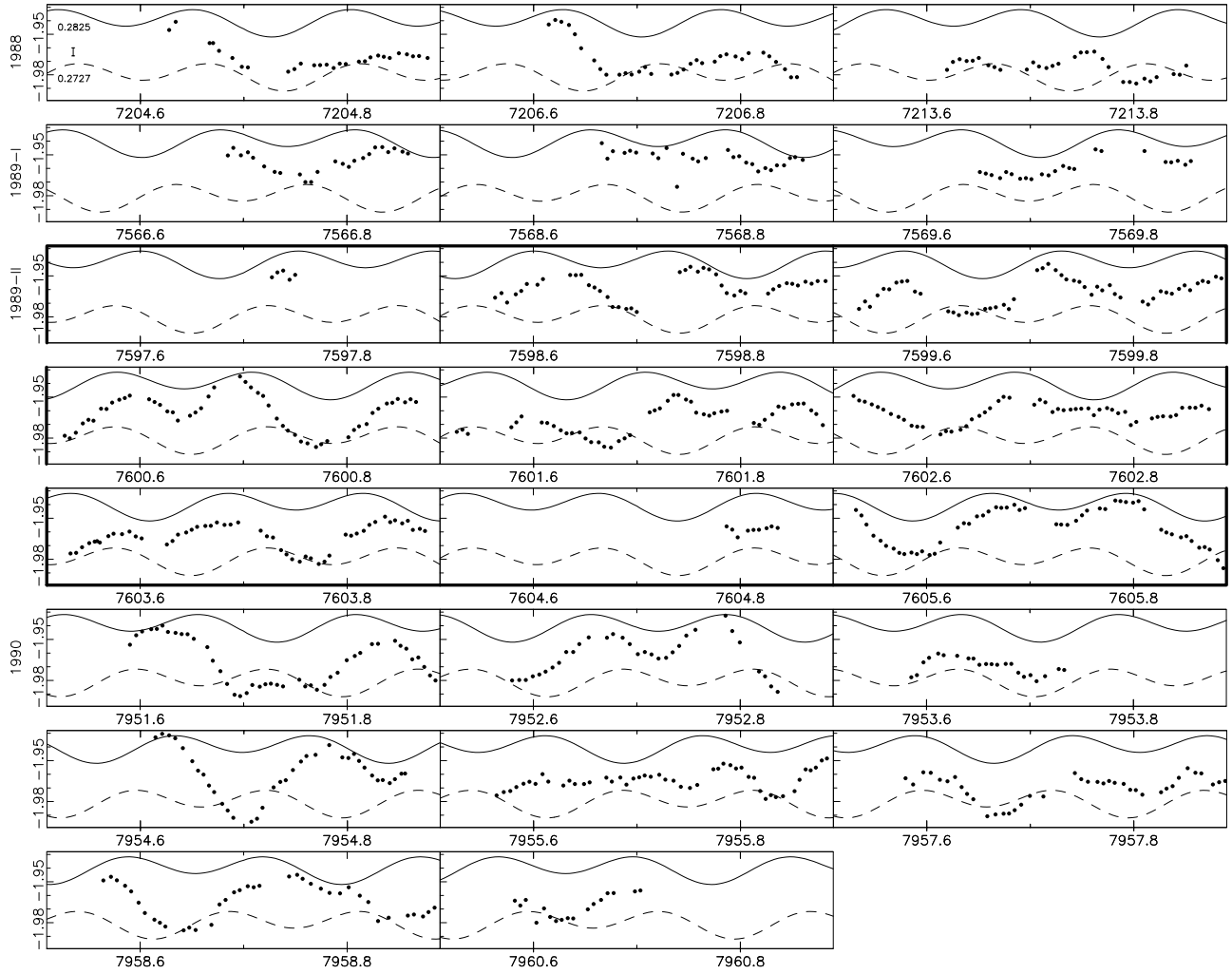


Fig. 1. Compilation of Walraven photometric light curves ($\log I$ versus HJD-24 40 000) of WR 46 obtained in 1988–1990. Bright is up. The standard deviation (± 0.003) of the comparison star is indicated by an error bar; the error of the differential magnitude is mostly as small as the size of the symbols. The solid and dashed curves represent synthetic double-wave light curves with a period 0.2825 d (top) and 0.2727 d (bottom). The curves are offset for a visual reason. The preferred curve is the solid one (see Sect. 4). The boldface margin indicates a large data set (Table 2 lists size of data sets).

In January and March 1999 the same set-up was utilized in the framework of the Long Term Photometry of Variables (LTPV) project (Sterken 1983; Sterken et al. 1995 and references therein). The Stromgren y -filter was utilized. It was possible to transform these data to the system of the 1998 V magnitudes because in two different nights a few measurements were practically simultaneously performed in both these filters. This data set will be discussed together with simultaneous spectroscopy by Marchenko et al. (2000; hereafter referred to as MAB), with whom we agreed only to present and discuss the periodogram (following section). The mean values are listed in Table 2 and displayed in Fig. 13.

3.4. V CCD photometry

One of us (WHA) obtained photometry using his private telescope (32 cm) with a ST 6 CCD attached, located in Marlborough, New Zealand. The telescope is located in a

vineyard at sea-level but with a low level of light pollution. Exposure times of the CCD were 50 s. The data were reduced on site. Differential photometry was obtained with respect to star “b”, and stars “c” and “d” were used as additional check (the letters refer to Fig. 4). After a successful test run in March 1999 (not presented), three nights of intense monitoring were obtained. Because of strong variability of the comparison stars presumably due to instability of the earth atmosphere, one night was rejected. The two resulting light curves are shown in Fig. 7.

4. Results

4.1. The frequency analysis

Figures 1–3, 5–7 present the observations in the various V -bands, except for the 1999-II data set which is displayed by MAB. Nights with only a few data points are not shown. The large variety in the shape of the cycles is striking. They vary from an ellipsoidal-type light

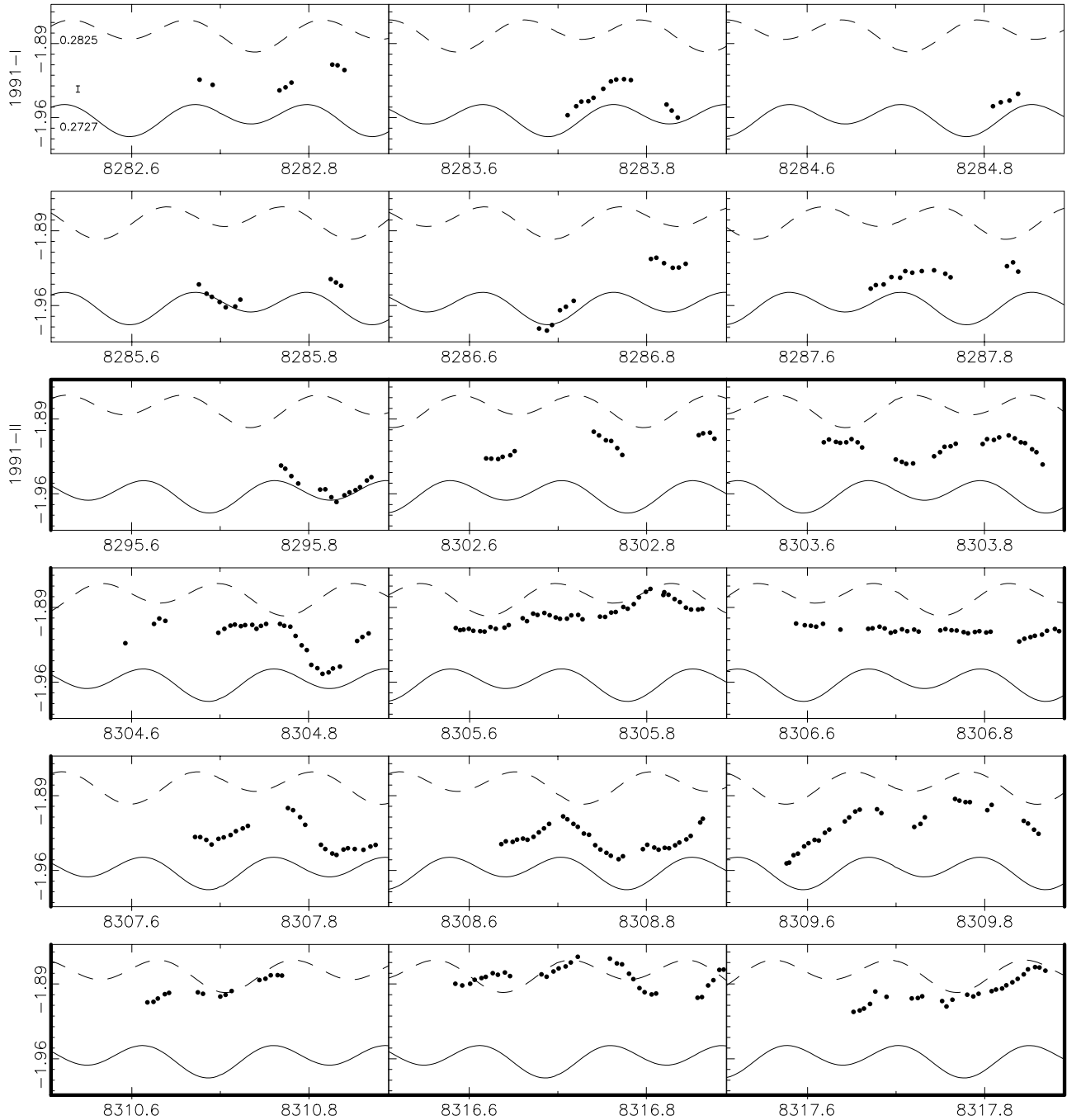


Fig. 2. The same as for Fig. 1, but now for 1991. Since the amplitude of variability is much larger, the diagrams are larger. Note, however, that the log I scale is off-set downwards compared to that of Fig. 1. The synthetic double-wave lower curve (solid) represents the 1991 data best.

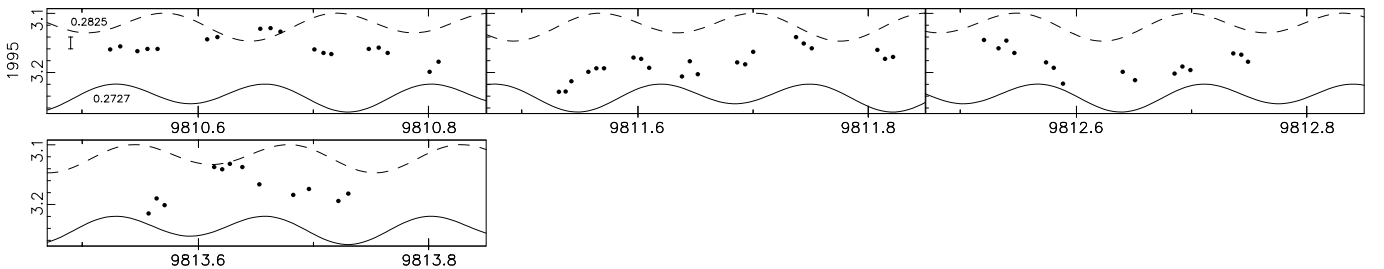


Fig. 3. Differential light curves in magnitudes of WR 46 with respect to HD 105150 in the ESO#99 V filter obtained in 1995. The typical error bar is indicated in the first panel.

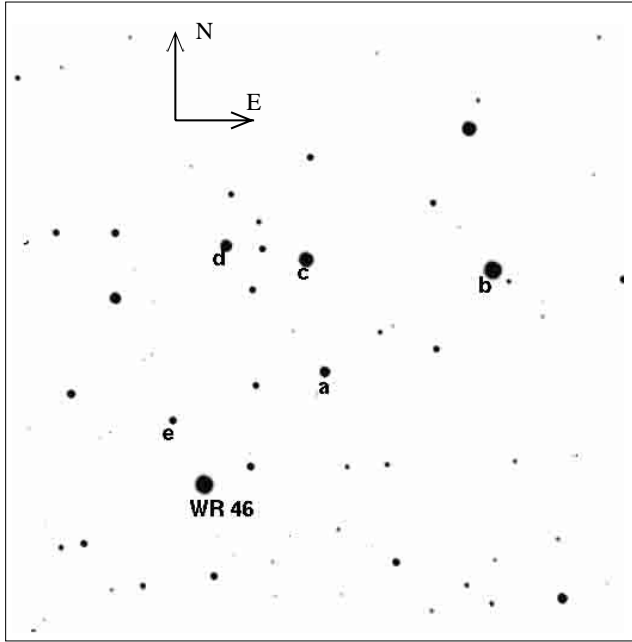


Fig. 4. An R filter CCD image ($3\farcm7 \times 3\farcm7$) of the field of WR 46. A larger area of the sky can be found in the finding chart in the catalogue by van der Hucht et al. (1981). The stars labeled “a” through “e” were used to perform differential photometry in 1998, and in 1999-III.

curve (HJD 2447600, with unequal maxima), to near constancy (HJD 2448306). They show either prolonged stages near minimum light (HJD 2447206, and HJD 2447951) or near maximum light (HJD 2448304). So, the light curve changes drastically from cycle to cycle. In addition, the mean magnitude of a cycle is variable too, sometimes by more than 0^m1 ($\log I = 0.04$), sometimes even from one night to the next (see HJD 2448304–8305).

Although this variability of the cycles hampers the use of any period search algorithm, we investigated the various data sets in the visual filters using several techniques. In general, the different techniques agree well and we focus our attention to the analysis of variance (AOV) (Schwarzenberg-Czerny 1989). This technique uses phase binning, but in contrast to the phase dispersion method by Stellingwerf (1978), its statistics is also well-defined for small samples. The expected value for a pure noise signal is 1, or, n_{corr} for observations correlated in groups of size n_{corr} . We used the AOV-routine within MIDAS, the ESO-reduction package. The large data sets are sufficiently extended to detect periods reliably. We note that the comparison star is carefully checked and the differential photometry of WR 50-C does not show any of the peaks discussed below.

4.1.1. The large data sets

The upper panel of Fig. 8 presents the AOV-periodogram of the 1989-II V data. A prominent peak related to the hourly variation can be identified at $f_{\text{sw}} = 7.08 \text{ cd}^{-1}$ (0.1412 d), where “sw” means “single-wave”.

Also indicated are its 1 cycle/day aliases (indicated as a_{sw}), and their sub-harmonics ($\frac{1}{2}f_{\text{sw}}$ and $\frac{1}{2}a_{\text{sw}}$). In addition, we notice a strong peak at $f_x = 4.34 \text{ cd}^{-1}$ (0.2304 d), with its 1/day aliases (a_x), where “x” means “unknown”. The spectral window (bottom panel) indicates that these frequency peaks are not due to windowing (power spectrum is clearly offset from integer number of cycles and ratio of peaks is very different). The periodogram of the $(V-W)$ color index is shown in the middle panel. Although from this panel alone it is not obvious which peak is the alias of which, it definitely confirms the single-wave frequency and its aliases and subharmonics. However, the frequency f_x is absent in the $(V-W)$ data, which means it is present in the V and W with equal light amplitudes, as is the case for the other continuum filters. We note that the double-wave period (= half frequency) is clearly present in the light variation, and is prominent in the color index. We note that the radial-velocity data (see Paper II) vary on a time scale of the double-wave period, though apparently not strictly periodic. Since also the folded light- and colour curves hint towards a double-wave structure, we will address that frequency specifically.

At this point we need to address the period identified by MAB of $P = 0.329(0.013) \text{ d}$, which has its first harmonic at 6.08 cd^{-1} . Although the latter frequency is present in our data too (see above), we consider the evidence from the light variations in our data strongly in favour of a frequency at 7.08 cd^{-1} . Convincing evidence for this frequency is found in the simultaneous spectroscopic data; the difference being that the radial velocity in subsequent nights is in phase in the data of MAB, while our data shows them to be in anti-phase. In addition, we note that their individual light curves show indication for a double-wave (see their Fig. 2) but the light curve folded with their period shows a single dip (their Fig. 1). However, those authors refrain from interpreting this light minimum because of a lack of phase coverage. Further discussion of their result is deferred to Papers II and III.

Figure 9 presents the same diagrams as in Fig. 8, but now for the 1991-II data set. Again, both the V data and the $(V-W)$ color indices clearly indicate a single-wave frequency $f_{\text{sw}} = 7.34 \text{ cd}^{-1}$, with its aliases and the subharmonics. The periodogram of 1989-II is drawn (grey) fitted within the panel. None of the large peaks of the 1989-II and the 1991-II periodogram coincide. However, the false-alarm probabilities (FAP¹) of all of the peaks mentioned above are smaller than 0.01. We point out that the width of the frequency peaks depends on the time span of the data, and that both the f_{sw} s are distinctly separated. Moreover, we repeated the analysis separately for the first half, and for the second half of both large data sets, and the same results emerge. Also correcting for the large night-to-night variations by subtracting the

¹ FAPs are based on a Fisher randomization test and represent the probability that the period is not equal to the identified value, but equal to some other value (Dhillon & Privett 1997).

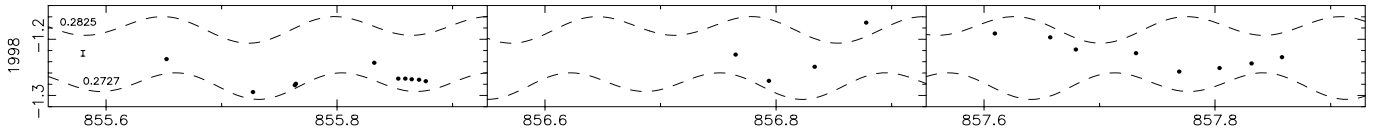


Fig. 5. Differential light curves (magnitudes versus HJD–24 50 000) of WR 46 relative to an ensemble of comparison stars in the field (see Fig. 4) in Bessel V in February 1998 (1998-I). The typical error bar is indicated in the first panel. As neither of the synthetic double-wave curves is preferred, both are shown dashed.

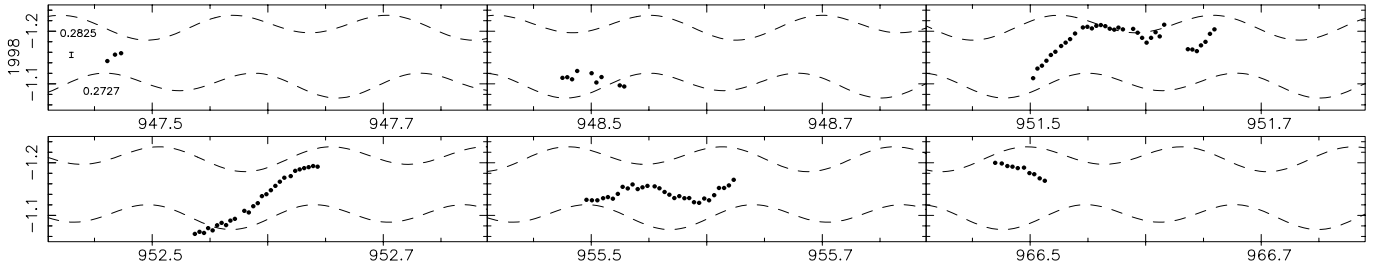


Fig. 6. As in Fig. 5, but for May 1998 data (1998-II).

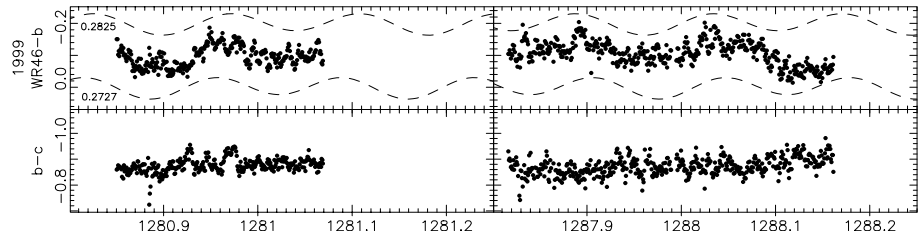


Fig. 7. Differential V_J light curves (magnitudes versus HJD-24 50 000) in April 1999 of WR 46 and of the primary comparison star relative to a secondary. The comparison stars are indicated using the labels as in Fig. 3. The vertical width of the light curve gives an impression of the uncertainty of the measurements.

mean intensity of each cycle, did not change the height or position of the various peaks. Furthermore, application of other period-search techniques (Fourier analysis, Scargle-Lomb periodograms) does not alter these results either. This significant difference of the period is most intriguing, as is the absence of a peak around f_x in 1991.

The frequency range up to the Nyquist frequency (around 70 cd^{-1} ; not shown) of the data sets does not show any evidence for additional periods, e.g., not at the sum frequency of f_x and f_{sw} . The low end in the 1989 periodogram shows decreasing power, but there is, in addition to some aliases, a minor peak at $f = 2.70 \text{ cd}^{-1}$ which happens to be close to the difference between f_{sw} and f_x . At the low frequency end, the 1991-II data set shows much more power than the 1989-II data set. This can be considered to be due to larger night-to-night variability in 1991. Actually, the highest peak for the 1991 data set lies at 0.23 cd^{-1} and 0.77 cd^{-1} (N.B. $0.77 = 1 - 0.23$) (with their one-day aliases). We consider it noteworthy that this frequency is equal to the reciprocal of f_x , but we do not know whether this reciprocity is relevant, or simply incidental.

Because of the circumstantial evidence, i.e., different minima and radial-velocity variability (Paper II), we suggest that the double wave is the true period. We present the double-wave periods of the 1989-II and the 1991-II

data sets:

$$P_{89} = 0^d 2825 \pm 0.0018 = 6^h 47^m$$

$$P_{91} = 0^d 2727 \pm 0.0006 = 6^h 33^m,$$

respectively. The uncertainties are derived from assuming a phase-error of 0.2 over the whole observing epoch divided by the number of cycles that elapsed. The difference of 14 min between the two double-wave periods is significant. The amplitudes and other periodicities are listed in Table 4.

We investigated the presence of f_x in the 1989-II data set by simulating the following double-wave light curve within the PERIOD-software of STARLINK (Dhillon & Privett 1997):

$$V(t) = A_1 \sin\left(\frac{2\pi}{P}t\right) + A_2 \sin\left(\frac{2\pi}{\frac{1}{2}P}t + \frac{\pi}{2}\right). \quad (1)$$

The quarter phase difference between the sine waves produces unequal minima and equal maxima. Generic white noise was added to the light curve. We selected points from this noisy constructed light curve according to the times of observation. Subsequently, this data set is subjected to the same analysis as described above. These constructed periodograms look quite similar to the observed periodogram (Fig. 8), except for the large peaks at the frequency f_x and its aliases, which are absent. Thus, we presume that this

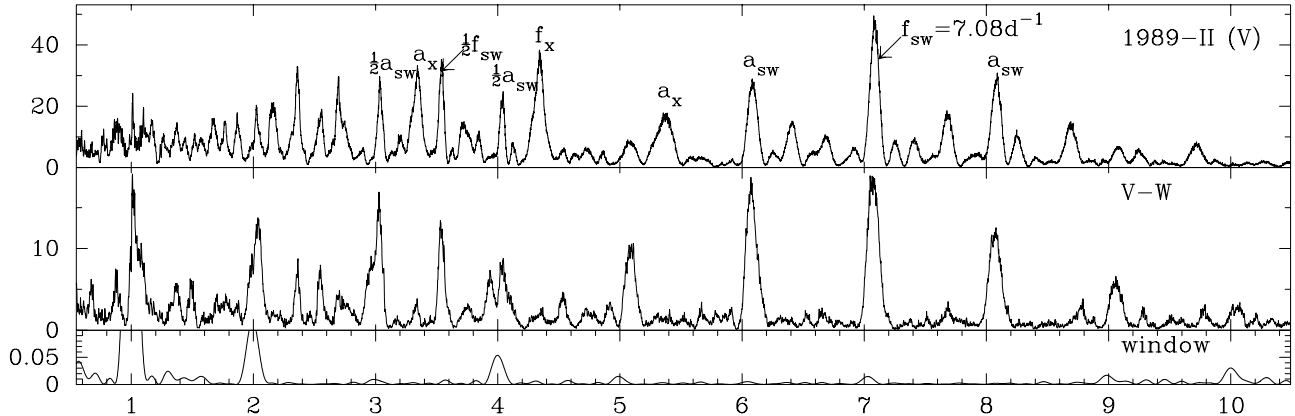


Fig. 8. The AOV periodograms (AOV statistic versus frequency in cd^{-1}) of the 1989-II V data set (top), $V - W$ (lower panel) and the Scargle-Lomb statistic for the spectral window (bottom).

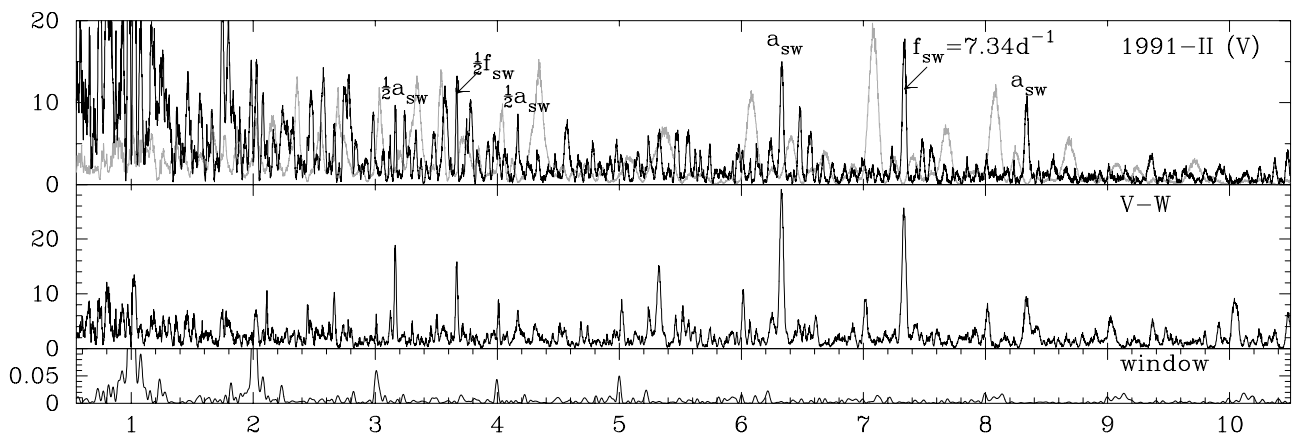


Fig. 9. As in Fig. 8, but now for 1991-II data-set. For comparison the 1989-II periodogram is shown in grey. It is evident that the two periods (with aliases and subharmonics) of these data sets differ significantly. Since the shapes of the accompanying light curves are similar, we suggest that the characteristic period of the system decreased by 3.5%.

frequency may indeed be intrinsic to WR 46, apparently without any colour variation. This frequency is not recovered from the 1991-II data, although there is an intriguing set of aliases at 3.59 , 4.59 , and 5.59 cd^{-1} . The difference between these peaks and f_x and its aliases equals the difference between the single-wave frequency in 1989-II and in 1991-II. We have no explanation for this coincidence.

4.1.2. The small data sets

In contrast to the extended data sets discussed above, the smaller data sets show an ambiguous frequency behaviour. Their frequency analysis does not result in a reliable period determination, which we attribute to small-number statistics and the high level of the additional variability from cycle-to-cycle. Nevertheless, we present their AOV periodograms in Fig. 10 in order to see whether any of the peaks coincide with the 1989-II or 1991-II periods, or the period by MAB f_{MAB} .

Table 5 lists the occurrence of the different frequencies as determined by MAB and in this paper (and Paper II). We can only conclude that these small data sets are not inconsistent with the periods as determined at other epochs.

Table 4. Periodicities in the large Walraven photometric data sets. The amplitudes A_{sine} and A_{whit} are determined by fitting a sine wave through the folded data, before and after prewhitening with the frequency indicated, respectively. The formal error from the fit is of the order 0.1 mmag. For the double-wave frequencies we list the depth of deep and the shallow minimum relative to the maximum. These depths have typically a mean error of 8 mmag, and a standard deviation of 25 mmag.

data set	id.	$P(d)$	(mmag)	(mmag)
1989-II	f_{sw}	0.1412	$A_{\text{sine}} = 21.3$	$A_{\text{whit}}^{f_x} = 20.0$
	f_x	0.2304	$A_{\text{sine}} = 16.8$	$A_{\text{whit}}^{f_{\text{sw}}} = 15.5$
	f_{dw}	0.2825	$A_{\text{deep}} = 45$	$A_{\text{shallow}} = 30$
1991-II	f_{sw}	0.1363	$A_{\text{sine}} = 28$	
	f_{dw}	0.2727	$A_{\text{deep}} = 73$	$A_{\text{shallow}} = 53$

However, we do not exclude the possibility that yet other frequencies controlled the variability.

We address the question whether the observations can be interpreted as a result of a rapidly-increasing clock rate. If so, we have to assume that the true period in the data by MAB is the one-day alias at 4.04 cd^{-1} , although those

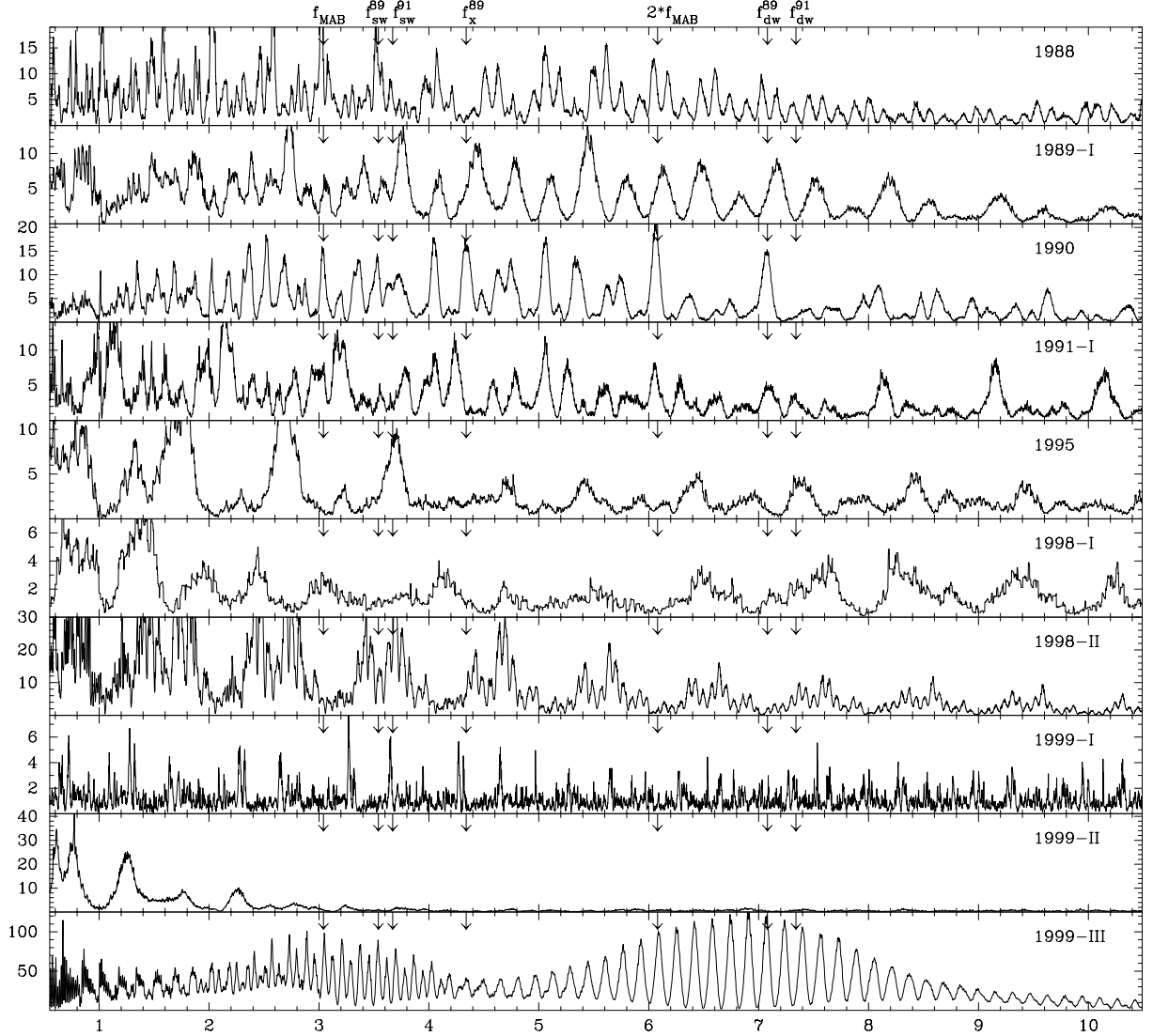


Fig. 10. The AOV periodograms (AOV statistic versus frequency in cd^{-1}) for the small data sets.

authors consider this alias unlikely though not impossible. On the basis of the small data sets it cannot be concluded that the data is inconsistent with an increasing clock-rate. If this view is correct, the clock rate seems not to change smoothly. The rate of change may be related to long-term brightenings of the object (See Sect. 4.3).

Summarizing the frequency analysis, it is evident that there is not a single clock with a constant rate underlying the photometric variability of WR 46, since the different periods in 1989 and 1991 are firmly established. Moreover, there is strong evidence for multi-periodicity because of the occurrence of a second period (f_x) in 1989 and 1990. Yet, the observations do not exclude the possibility that the dominant variation, which also affects the ($V-W$) colour index, is controlled by a single clock with a rapidly varying (increasing) clock-rate.

4.2. Folded light- and colour curves

To investigate the difference between the 1989-II and 1991-II periods, we fold all the photometric data with both

periods. Figure 11 (left) shows all V data folded with the longer 1989-II period and, (right), folded with the shorter 1991-II one. We use for each season a separate zero point T_0 (see Table 2) for the computation of the phases, since the large gaps between the data sets, and the change of the apparent period prevent the determination of one single ephemeris. We have chosen the zero points such that the data sets display, where possible, a deep minimum at phase zero. We note that the boxes neighbouring the fat boxes show that in both cases the period of the other data set should be rejected, confirming the change of the period. This is substantiated by folding the colour curves ($V-W$) using the “wrong” period (Fig. 11), which is even more convincing.

Figure 12 displays the light- and colour-curves of the two extended data sets 1989-II and 1991-II, each folded with their own double-wave period. The double-wave character is apparent, and its significance is investigated below. The typical colour behaviour, i.e., red when bright, is also evident. Due to the relatively large changes in mean brightness and amplitudes, the vertical scale of the

Table 5. Peaks in the aov-periodograms of the small data sets consistent with determined frequencies.

set	$f_{\text{MAB}}^{\text{rv}}$	f_{sw}^{89}	f_{sw}^{91}	f_x	$2*f_{\text{MAB}}$	f_{dw}^{89}	f_{dw}^{91}
1988	++	++	+			++	
1989-I					+		
1990	++	++		++	++	++	
1991-I	+				++	+	
1995			++				+
1998-I							
1998-II		+	++	+			+
1999-I			++	+			
1999-II							
1999-III	++	++			++	++	

1991-II light curves is shifted downward by $\log I = 0.045$ and reduced by a factor 1.6 compared to that of 1989-II. The scales for the colour curves in the bottom half of Fig. 12 are equal for both data sets. Apart from the usual colours ($V-B$), ($B-L$), ($B-U$), and ($U-W$), also ($V-W$) is shown. The latter colour index spans the largest wavelength range, and represents therefore the largest colour changes. In constructing the 1991-II light curve, we removed the rising trend of about $0^m 1$ as can be observed in Fig. 2 and in the insert in Fig. 13. The white-on-black curves have been constructed as running means over a phase interval of $\Delta\phi = 0.06$, with steps of 0.03 in phase.

The depths of the deep and the shallow minima are listed in Table 4. We applied the Student's t test (Press et al. 1986) to a phase interval 0.1 around both minima. The observed differences in 1989 of $0.005 \log I$ and in 1991 of $0.009 \log I$ are this large (or larger) by chance, are 26% and 38%, respectively, after correction for the correlation of the data points within one night. The shallow minimum of the 1989-II data is bluer by $0.003 \log I$ than the deep minimum. The chance that this is accidental is 7%.

These corrected percentages cannot be considered as convincing evidence that the light minima differ. However, effectively we have measured the difference twice (once in 1989 and once in 1991). Thus, we may multiply the probabilities, and find that there is 10% chance that one finds such a large difference between the two minima twice by chance. We conclude that there is strong photometric evidence that the true period is twice the single wave period. Note that our spectroscopy confirms this thesis (see Paper II).

To characterize the variability we note that its time scale is of order 0.3 d. Furthermore, the multi-colour photometry shows the object to persist in its colour behaviour (redder when brighter, i.e., a larger amplitude towards the red), which is substantiated by the variances around the mean as listed in Table 3. Moreover, this colour behaviour is also found in the observations by MAB. Discussion of the changes of the periods determined here and the one by MAB is deferred to Paper III.

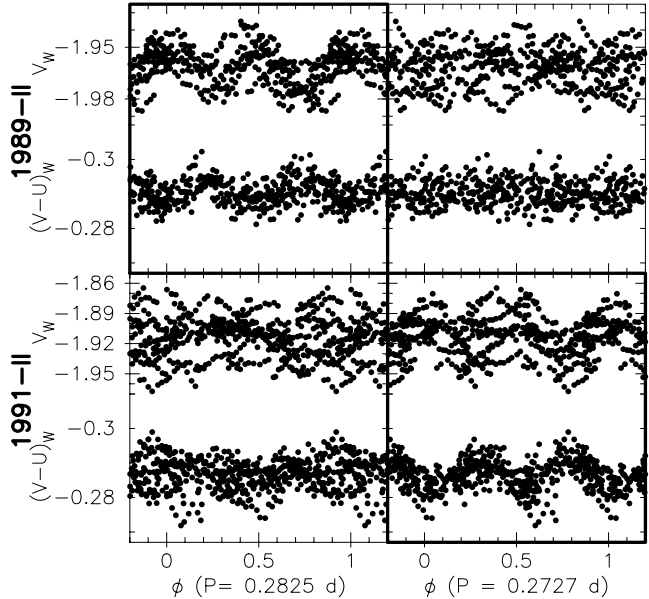


Fig. 11. The large data sets 1989-II and 1991-II are folded with both the periods as determined in these data sets. The period in 1989 is clearly not applicable to the data, especially in the color $V - U$ in 1991 and vice versa. This illustrates that the period of WR 46 did vary between 1989 and 1991.

4.3. The long-term photometric variation

Figure 12 illustrates, in addition to the change of the period, the double-wave nature, and the colour behaviour, also the long-term light- and colour variation between 1989 and 1991. First of all, the object was brighter in 1991 by about $0^m 12$ ($=0.048 \log I$ in Table 2). Hereby, we confirm the long-term photometric behaviour of WR 46 as revealed by the *Hipparcos* satellite (Marchenko et al. 1998). These authors noted that its brightness increased from 1989 to a maximum $\Delta H_p \simeq 0^m 25$ by the end of 1991 and decreased to the 1989-brightness in the course of 1993 (see Fig. 13). We note that the brief excursion on JD = 2448312 is in line with the almost simultaneous Walraven photometry (see insert in Fig. 13).

Secondly, the mean amplitude of the light curve is larger in 1991 by roughly a factor 1.7 (note the difference in the right- and left hand side ordinate scale in Fig. 12). Furthermore, also the scatter around the mean light curves caused by the differences from cycle to cycle, increased roughly by a factor 1.6, while the scatter around the colour curves increased only by a factor of 1.2. We note that except for these changes, the character of the variability, or the general shape of the light curve did not change. Both the unequal minima, although only marginally significant, and the colour behaviour persisted during those years.

The mean colours changed as can be seen in Fig. 12, though at most by $0^m 020$. It appears that the line emission can explain the intricate up- and downwards changes of the mean colours. We produced an average spectrum of each spectral monitoring data set and folded this with

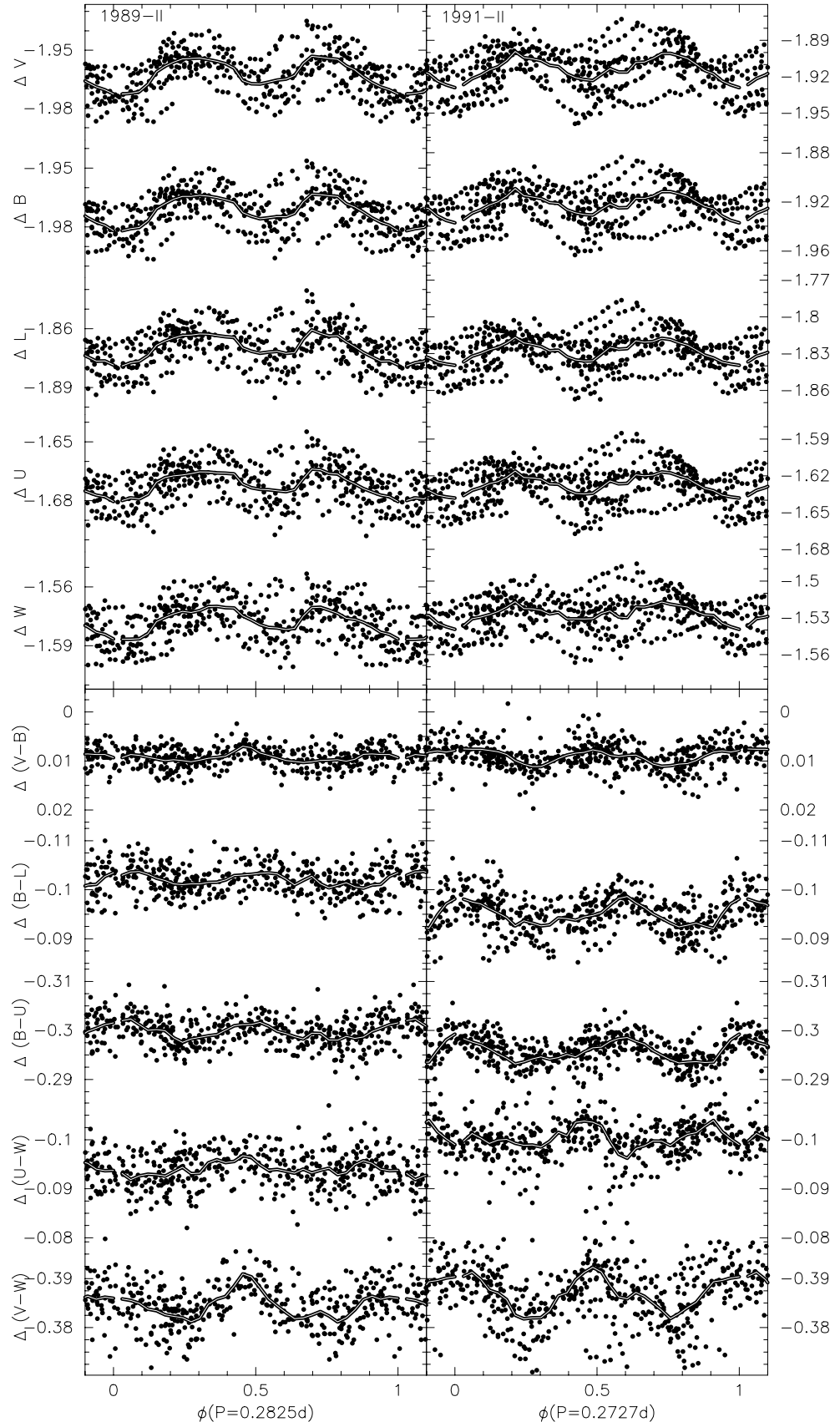


Fig. 12. The folded light (upper 5 curves; bright is up) and colour variations (lower 5 curves; blue is up) of the two largest data sets are displayed ($\log I$ scale). The vertical scales of the top five panels to the right are off-set downward by 0.045 $\log I = 0^m 12$, and enlarged by a factor 1.6. The accompanying colour variations (lower curves) have identical vertical scales (left and right) but are enlarged by a factor of 3 compared to those of the light curves.

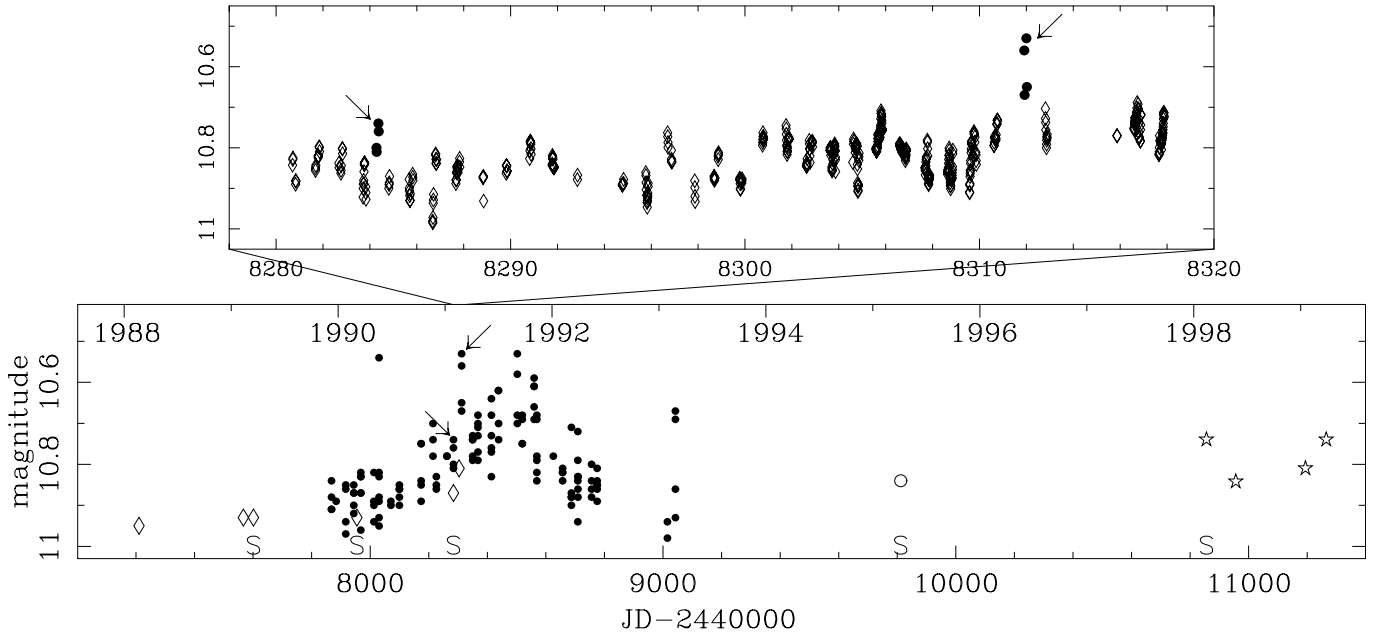


Fig. 13. The lower panel shows the *Hipparcos* photometry (H_p : 1989–1993) of WR 46 as dots. The open lozenges are the means from three monitoring observing runs using the Walraven photometer. The offset between the two systems is due to the differences in filter. The epochs of simultaneous spectral monitoring are indicated with “S”. The insert (above) presents the individual Walraven data points in Feb./March 1991. Note that the excursion from JD 2448284 to JD 2448312 of the H_p magnitudes (see arrows) is in line with the Walraven photometry. The difference in amplitude of the change and the excursion is attributed to the larger contribution of line flux to H_p -pass band. In addition, the photometric means of 1995 (open circle) relative to 1998 and of 1998 and 1999 (open stars) are indicated.

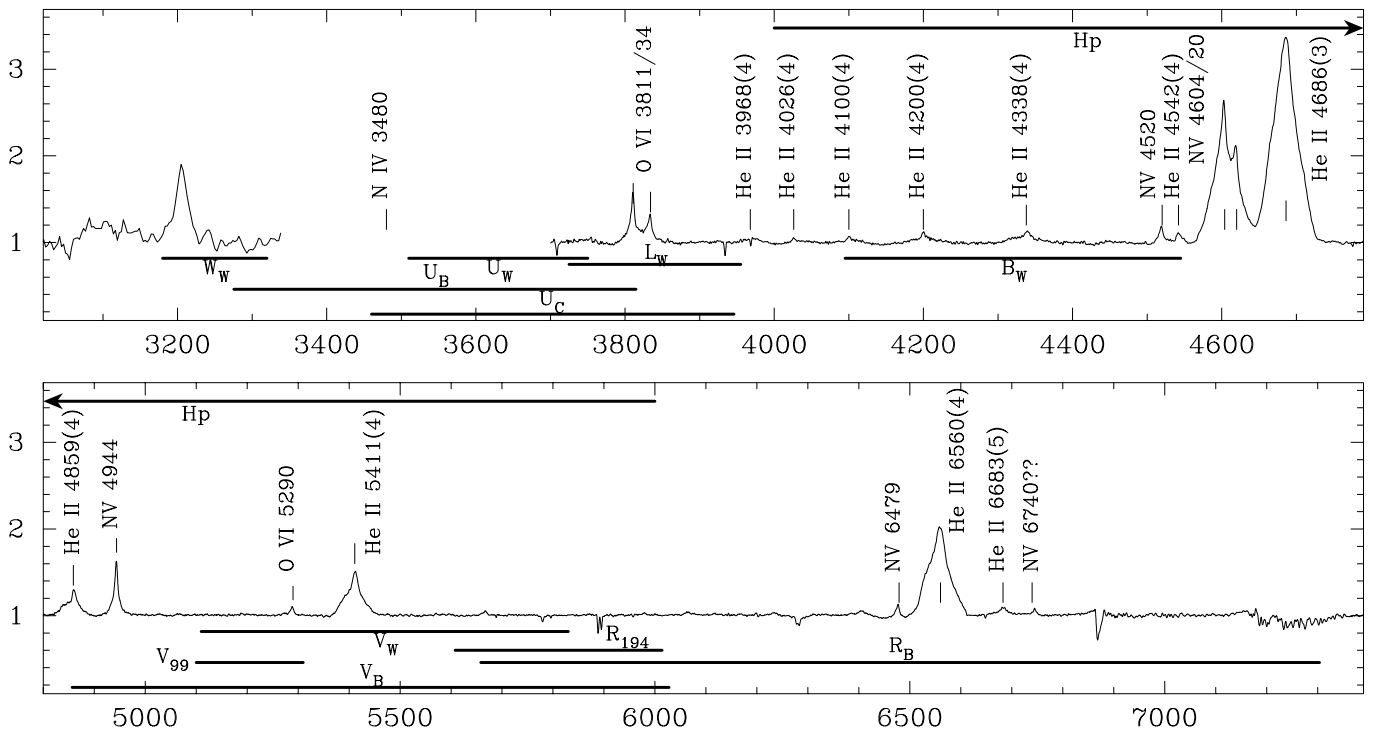


Fig. 14. The spectrum of WR 46 (Hamann et al. 1995b) with the FWHM indicated for the respective pass bands used in the present paper. As to the wavelength range not covered by the spectrum, the N IV 3480 Å line could be present according to Smith et al. (1996). The spectrum by Massey & Conti (1983) does display the line significantly, while that of Smith (1955) does not show any sign of this emission line. The He II 3203 (5–3) line has been detected in 1991 by *IUE* (image number LWP10528) at almost twice the continuum flux. The emission-line contribution to the different pass bands is obvious.

Table 6. The mean line emission contribution (as percentage of the received fluxes) to the Walraven V , B , and L pass bands, and to the *Hipparcos* pass band. Clearly, the line fluxes contributed more in 1991 than in 1989 to the various pass bands, showing that the emission lines grew even stronger than the rise of the continuum. Due to the periodic short-term variations of the spectra (lines plus continuum), the percentages vary by about 10%.

year	V	B	L	H_p
1989	2.6	5.0	–	~8
1991	3.7	7.0	3.1	~12

the pass-bands covering the sampled spectral range (see Fig. 14). Table 6 lists the results for 1989 and 1991. Because of the larger increase of line contribution to the B -pass-band (2%) than the V -pass-band (1%), the object should become bluer in $(V-B)$, while this colour index remained constant. Apparently, the continuum emission has reddened by 1% ($0.^m01$) to produce constant colour index. The other colour indices are consistent with such a small reddening, considering the various changing emission-line contributions. The $(B-L)$ index is $0.008 \log I$ ($=0.^m020$) larger (redder), $(U-W)$ is smaller by $0.005 \log I$ (bluer by $0.^m013$), while the $(V-W)$ did not change significantly, probably due to an increase of the O VI 3811–34 line complex (no spectral coverage in 1989).

Furthermore, we note that the contamination by emission lines of the *Hipparcos* pass band increased considerably more ($\sim 4\%$) than the Walraven V band ($\sim 1\%$), thus explaining the larger rise in brightness ($\sim 3\%$) as observed by the satellite. Altogether, this implies that, while the continuum rose, the line flux increased even more. For instance, the line flux of the large line complex of N V 4603/19 and He II 4686 increased by roughly 60%, as the EW -measurements show (see Paper II).

Figure 13 presents an overview of the mean magnitudes of all observed seasons. The differences should be considered with caution when observed using different photometers (different symbols). Yet, from Table 2 it is apparent that the mean magnitude decreased $0.^m10$ between February 1998 and May 1998 (see also Table 3). In 1999, the system appears to brighten by $0.^m07$ from January to April. The 1995 mean brightness is computed relative to the same comparison star as in 1998 and appears to be at a rather low photometric level. In addition, there is a hint of a rising trend over the whole decade, however its significance cannot be investigated because of the use of different instrumentation. Moreover, the observations as listed in Table 1 are inadequate to investigate its photometric behaviour over the last century. This issue will be re-addressed using the available spectra (Paper II).

The long-term brightening of WR 46 is unique among WR stars in the *Hipparcos* survey of 67 such stars (Marchenko et al. 1998). Furthermore, assuming that the long-term light curve is not sinusoidal but better described as a single event (possibly recurrent), we do not recognize

the shape of the light curve as characteristic for a specific phenomenon, e.g., it does not look like S Dor- (LBV)-pulsations (WR stars are supposed to be descendants of S Dor variables), nor does it resemble long-term behaviour of Super Soft Sources, or that of V Sge (Šimon & Mattei 1999), an object to which WR 46 has been erroneously suggested to be related (Paper II).

In summary, we suggest that on a time scale of months to years WR 46 shows irregular cycles with an amplitude amounting up to $\sim 0.^m3$. Our photometry confirms the brightening in 1991 and suggests that another brightening occurred in the course of 1997 and a third one peaking in the year 1999 or 2000. We suggest that the period change from 1989 to 1991, the possible slight reddening, and the change of amplitude is related to the so-called *Hipparcos*-brightening. If so, the incompatibility of the 1998 and 1999 data with P_{89} and P_{91} may be related to the brightenings in those years.

5. Summary

The photometric observations of WR 46 can be summarized as follows, with respect to its short-term variability:

1. the periodograms display a dominant frequency $P_{sw} = 0.14$ d,
2. the light curve shows probably a double wave with unequal minima of *on average* a deep minimum of $\sim 0.^m04$ – $0.^m07$ and a shallow minimum of $0.^m03$ – $0.^m05$,
3. an additional frequency (f_x) occurs in 1989 within one large data set (1989-II),
4. the frequency spectrum of the colour variability only reveals f_{sw} , with its aliases and (sub-)harmonics,
5. its colour turns red when bright and blue when faint,
6. the colour curve in 1989 indicates that the shallow minimum is possibly bluer than the deep minimum,

and, with respect to its long-term variability:

7. peculiar irregular cycles occur up to $0.^m3$ unique among WR stars,
8. at least one long-term brightening was accompanied by a slight reddening,
9. possibly, the long-term brightenings are related to changes of the dominant frequency (f_{sw}); at least for the one well-observed case in 1991 we find:
 - a significant change of 3.5% of the (colour)-dominating frequency on the rising branche of the brightening. Although the brightness probably returned to its original level, the 1995 data suggest that the frequency change persisted,
 - the amplitude of the short-term variability increased by a factor 1.7.

As mentioned in Sect. 2, the spectrum of WR 46 has been alternatively interpreted as resulting from an accretion disc (Niemela et al. 1995; Steiner & Diaz 1998). However, in Paper II we discuss that the colour behaviour is consistent with the continuum emerging from a hot star, and

that the WR nature is strongly supported by its spectroscopic variability, in agreement with the conclusions by MAB.

We conclude that the short-term variability can be understood either as a dominant mechanism controlling the light *and* colour and, possibly, radial-velocity variations (Paper II), which changes its frequency within years (a clock with variable clock-rate), while an additional frequency may affect the brightness. Or, the object can show various modes with different frequencies. In both cases the link with the mean optical brightness may be intrinsic: a true change of a clock rate may be accompanied by a brightening, and a mode switch may be related to brightness changes. Interpretation of these observations in terms of a model are deferred to Paper III.

Acknowledgements. We thank Martha Hazen for searching the plate archive of the Harvard Observatory for all early plates of WR 46. We gratefully acknowledge the observational effort performed by Albert Jones, monitoring on a nearly daily basis many visible WR stars on the southern hemisphere. The observations suffer from a yearly modulation, though show convincingly that WR 46 does not show large rapid variations. We also thank the many observers, some of them students at the time, and the “lovers” (=amateurs) who spent their free time at their telescopes. The extended comments by the referee, Tony Moffat, have helped to improve the paper. This research has made use of the Simbad database, operated at CDS, Strasbourg, France. C.S. and T.A. acknowledge financial support from the Fund for Scientific Research Flanders.

References

- Cannon, A. J. 1916, Annals Harvard College Observatory, vol. 76(3), 19
- Crowther, P. A., Smith, L. J., & Hillier, D. J. 1995, A&A, 302, 457 (CSH)
- Dhillon, V. S., & Privett, G. J. 1997, Starlink User Notes, 167.5
- Duijsens, M. F. J., van der Hucht, K. A., van Genderen, A. M., et al. 1996, A&AS, 119, 37
- Fleming, W. P. 1910, Harvard College Observatory Circ., 158
- Fleming, W. P. 1912, Annals, Harvard College Observatory, 56, VI, 165
- van Genderen, A. M., van der Hucht, K. A., & Larsen, I. 1990, A&A, 229, 123
- van Genderen, A. M., Verheijen, M. A. W., van Kampen, E., et al. 1991, in Wolf-Rayet Stars and Interrelations with Other Massive Stars in Galaxies, ed. K. A. van der Hucht, & B. Hidayat, IAU Symp., 143 (Kluwer, Dordrecht), 129
- de Geus, E. J., Lub, J., & van de Grift, E. 1990, A&AS, 85, 915
- Hamann, W.-R., Koesterke, L., & Wessolowski, U. 1995a, A&A, 299, 151
- Hamann, W.-R., Koesterke, L., & Wessolowski, U. 1995b, A&AS, 113, 459
- Hamann, W.-R., & Koesterke, L. 1998, A&A, 333, 251
- Henize, G. H. 1976, ApJS, 30, 491
- van der Hucht, K. A. 2001, New Astron. Rev., 45, 135
- van der Hucht, K. A., Cassinelli, J. P., Wesselius, P. R., & Wu, C.-C. 1979, A&AS, 38, 279
- van der Hucht, K. A., Conti, P. S., Lundström, I., & Stenholm, B. 1981, Space Sc. Rev., 28, 227
- Lub, J., & Pel, J. W. 1977, A&A, 54, 137
- Lynga, G., & Wramdemark, S. 1973, A&AS, 12, 365
- Marchenko, S. V., Moffat, A. F. J., van der Hucht, K. A., et al. 1998, A&A, 331, 1022
- Marchenko, S. V., Arias, J., Barbà, R., et al. 2000, AJ, 120, 2101 (MAB)
- Marston, A. P., Chu, Y. H., & Garcia-Segura, G. 1994, ApJS, 93, 229
- Massey, P., & Conti, P. S. 1983, ApJ, 264, 126
- Monderen, P., de Loore, C. W. H., van der Hucht, K. A., & van Genderen, A. M. 1988, A&A, 195, 179
- Münch, L. 1953, Bol. Obs. Toantintla y Tacubaya 1(8), 27
- Niemela, V. S., Barbà, R. H., & Shara, M. 1995, in Wolf-Rayet Stars: Binaries, Colliding Winds, Evolution, IAU Symp., 163, ed. K. A. van der Hucht, & P. M. Williams, (Kluwer, Dordrecht), 245
- Payne, C. H. 1930, Harvard Observatory Monograph No. 3, Chapter 6
- Pel, J. W. 1986, Internal Report, Leiden Obs.
- Press, W. H., Teukolsky, S. A., Vetterling, W. T., & Flannery, B. P. 1986, Numerical Recipes (Cambridge University Press), 609
- Roberts, M. S. 1962, AJ, 67, 79
- de Ruiter, H. R., & Lub, J. 1986, A&AS, 63, 59
- Scargle, J. D. 1982, ApJ, 263, 835
- Schmutz, W., Hamann, W.-R., & Wessolowski, U. 1989, A&A, 210, 236
- Schwarzenberg-Czerny, A. 1989, MNRAS, 241, 153
- Simon, V., & Mattei, J. A. 1999, A&AS, 139, 75
- Slawson, R. W., Hill, R. J., & Landstreet, J. D. 1992, ApJS, 82, 117
- Smith, H. J. 1955, Thesis Harvard College Observatory, 130 (Abstract see AJ 60, 180)
- Smith, L. F. 1968a, MNRAS, 138, 109
- Smith, L. F. 1968b, MNRAS, 140, 409
- Smith, L. F., Shara, M. M., & Moffat, A. F. J. 1996, MNRAS, 281, 163
- Steiner, J. E., & Diaz, M. P. 1998, PASP, 110, 276
- Stellingwerf, R. F. 1978, ApJ, 224, 953
- Stephenson, C. B., & Sanduleak, N. 1971, Luminous Stars in the Southern Milky Way, Publ. Warner and Swasey Obs., 1, 1
- Sterken, C. 1983, ESO Messenger, 33, 10
- Sterken, C., Manfroid, J., Beelen, D., et al. 1995, AAS, 113, 31
- Torres-Dodgen, A. V., & Massey, P. 1988, AJ, 96, 1076
- Veen, P. M., van Genderen, A. M., Verheijen, M. A. W., & van der Hucht, K. A. 1995, in Wolf-Rayet Stars: Binaries, Colliding Winds, Evolution. IAU Symp., 163, ed. K. A. van der Hucht, & P. M. Williams, (Kluwer, Dordrecht), 243
- Veen, P. M., & Wieringa, M. 2000, A&A, 363, 1026
- Veen, P. M., van Genderen, A. M., van der Hucht, K. A., & Jones, A. 1999, in ed. K. A. van der Hucht, G. Koenigsberger, P. R. J. Eenens, Wolf-Rayet phenomena in Massive Stars and Starburst Galaxies, IAU Symp., 193, 263
- Veen, P. M., van Genderen, A. M., Crowther, P. A., & van der Hucht, K. A. 2002a, A&A, 385, 600 (Paper II)
- Veen, P. M., van Genderen, A. M., & van der Hucht, K. A. 2002b, A&A, 385, 619 (Paper III)
- Verheijen, M. 1991, Internal Report, Leiden Observatory
- Westerlund, B. E., & Garnier, R. 1989, A&AS, 78, 203
- Wilson, E. B., & Luyten, W. J. 1925, Harvard Reprint, 11(2), 134